Supporting Information

A diketopyrrolopyrrole-based small molecule with extended conjugated skeleton and J-aggregation property for 808 nm laser triggered phototheranostics

Jiawei Liu,[a] Xinmin Zhang,[a] Mingxuan Fu,[a] Xiaoyuan Wang,[a] Yicong Gao,[a] Xingpeng Xu,[a] Tangxin Xiao,[b] Qi Wang*[a] and Quli Fan*[a]

[a] State Key Laboratory for Organic Electronics and Information Displays & Institute of Advanced Materials (IAM), Nanjing University of Posts & Telecommunications, Nanjing 210023, China. E-mail: iamqwang@njupt.edu.cn, iamqlfan@njupt.edu.cn.

[b] School of Petrochemical Engineering, Changzhou University, Changzhou, 213164, China.

Table of Contents

1. Materials and apparatus

All reactions were performed in atmosphere unless noted. The commercially available reagents and solvents were either employed as purchased or dried according to procedures described in the literature. All materials about cell experiments were obtained from Nanjing KeyGen Biotech. Co. Ltd. Other materials were obtained from Sigma-Aldrich. ^{1}H NMR spectrum was tested on a Bruker AVANCE III instrument. The matrix-assisted laser desorption/ionization time-of-flight (MALDI-TOF) mass spectra were measured by a Bruker Autoflex TOF/TOF spectrometer. The morphology and size of NPs were determined by a HT7700 transmission electron microscope (TEM) and a particle size analyzer (Brookhaven Instruments), respectively. Absorption and emission spectra were obtained using a UV3600 UV/vis/NIR spectrophotometer (Shimadzu) and an NIR-II spectrophotometer (Fluorolog 3, Horiba), respectively. The MTT experiments were conducted using a microplate reader (Bio-Rad Laboratories, Hercules). The flow cytometry experiments were conducted through a Flow Sight Imaging Flow Cytometer (Merck Millipore, Darmstadt, Germany). The NIR-II fluorescence in vivo imaging were performed with InGaAs array detector (Princeton Instruments, NIR vana 640) equipped 980 nm long-pass filter. The exposure time for in vivo imaging was 200 ms. The 8 weeks old female Balb/c nude mice were used in the animal experiment. All animal procedures were performed in accordance with the Guidelines for Care and Use of Laboratory Animals of KeyGEN BioTECH and approved by the Animal Ethics Committee of Simcere BioTech Corp., Ltd.

2. *Synthesis of DPP-OPIC*

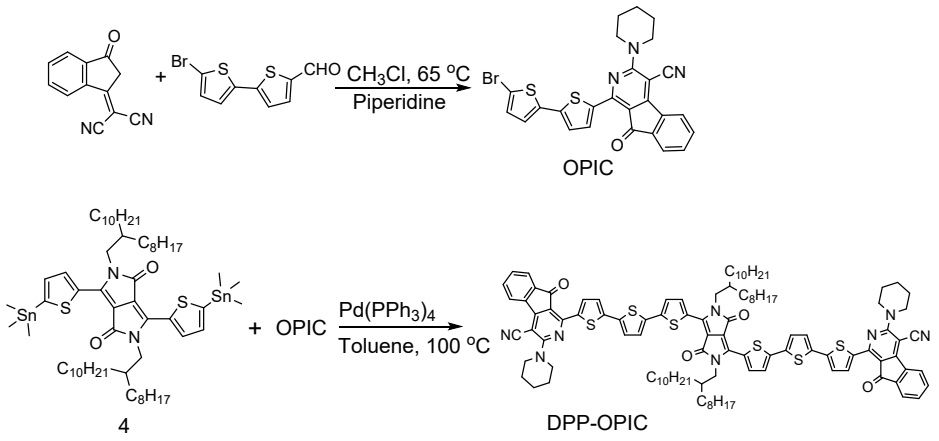

Scheme S1. Synthesis of DPP-OPIC.

Synthetic route of compound OPIC:

5'-bromo-[2,2'-bithiophene]-5-carbaldehyde (100 mg，0.51 mmol), 1-(5'-bromo-[2,2'-bithiophen]-5-yl)-9-oxo-3-(piperidin-1-yl)-9H-indeno[2,1-c]pyridine-4-carbonitrile (140 mg，0.51 mmol) and 0.5 mL piperidine were put into a double-necked flask, and nitrogen was bubbled three times to make the reactant in a nitrogen atmosphere. Then anhydrous 10 mL $CHCl_3$ was injected into reaction solution. The mixture was stirred and refluxed for 8 h at 65 °C. After the completion of the reaction, the reaction solution was cooled to room temperature, and the reaction solvent was removed through steps such as extraction and rotary evaporation. Finally, a dark yellow compound OPIC was obtained by column chromatography. (240 mg, 0.45 mmol, 88%). ^{1}H NMR (400 MHz, $CDCl_3$) δ 9.06 (d, 1H), 8.40 (d, 1H), 7.76 (d, 1H), 7.63-7.53 (m, 2H), 7.18 (d, 1H), 7.07 (d, 1H), 7.01 (d, 1H), 3.96 (br., 4H), 1.80 (br., 6H). MALDI-TOF: m/z calcd. for $C_{26}H_{18}BrN_3OS_2$, 532.474; Found: 532.362.

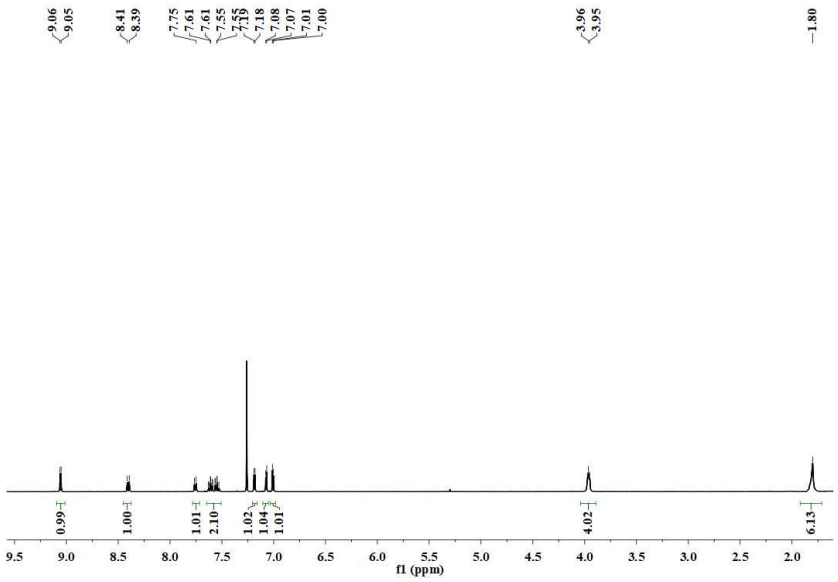

Fig. S1. [1]H NMR spectrum of OPIC.

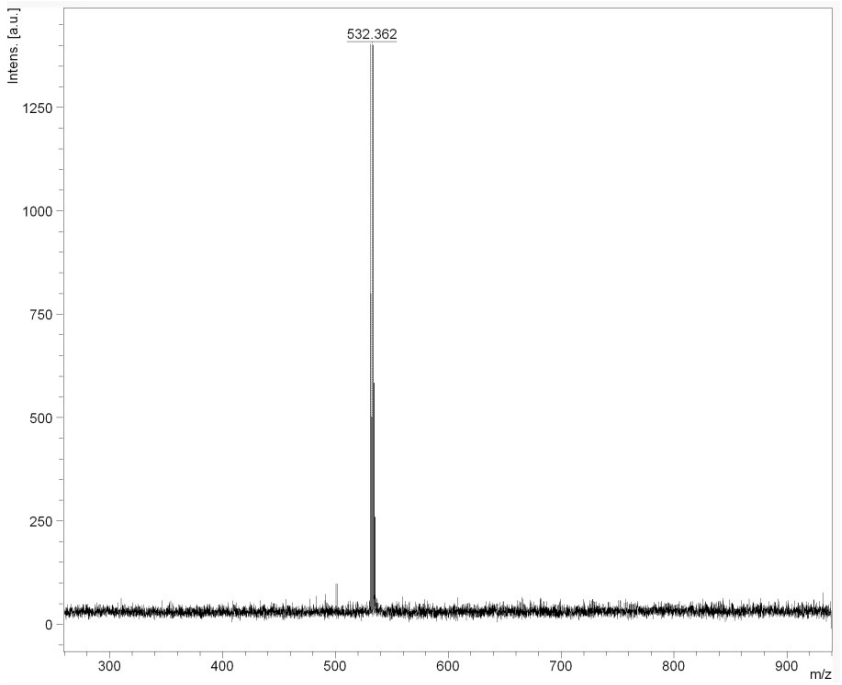

Fig. S2. MOLDI-TOF-MS spectrum of OPIC.

Synthetic route of compound DPP-OPIC:

Under nitrogen protection, 2,5-bis(2-octyldodecyl)-3,6-bis(5-(trimethylstannyl)thiophen-2-yl)-2,5-dihydropyrrolo[3,4-c]pyrrole-1,4-dione (50 mg, 0.042 mmol), compound OPIC (45 mg，0.085 mmol), tetrakis(triphenylphosphine) palladium (5 mg, 0.0043 mmol) were put into a double-necked flask. Then, toluene solvent (10 mL)

was added to reflux at 100 °C, and the reaction was performed in the dark for 24 h. The reaction solvent was removed by extraction, rotary evaporation. Finally, the dark green solid compound DPP-OPIC was obtained by column chromatography. (50 mg, 0.028 mmol, 67%). ^{1}H NMR (400 MHz, $CDCl_3$) δ 7.69-7.65 (m, 8H), 7.57-7.53 (m, 4H), 7.49-7.45 (m, 8H), 3.99 (br., 4H), 2.04 (br., 2H), 1.89-1.79 (m, 4H), 1.68-1.59 (m, 16H), 1.42-1.09 (m, 58H), 0.89-0.79 (m, 18H). MALDI-TOF: m/z calcd. for $C_{106}H_{122}N_8O_4S_6$, 1762.791; Found: 1763.126.

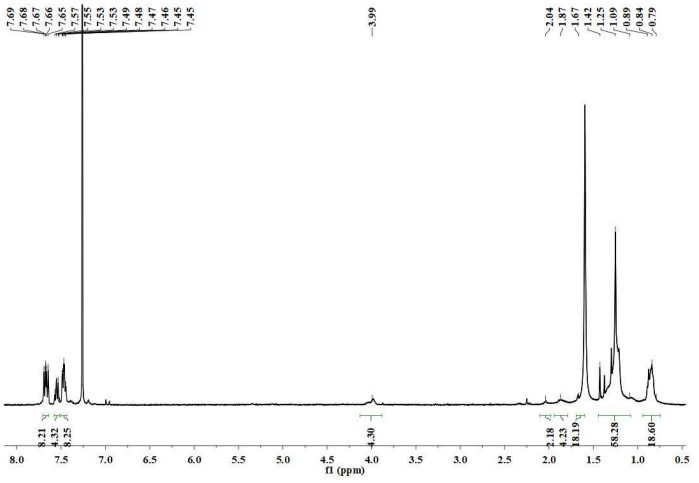

Fig. S3. ^{1}H NMR spectrum of O-T.

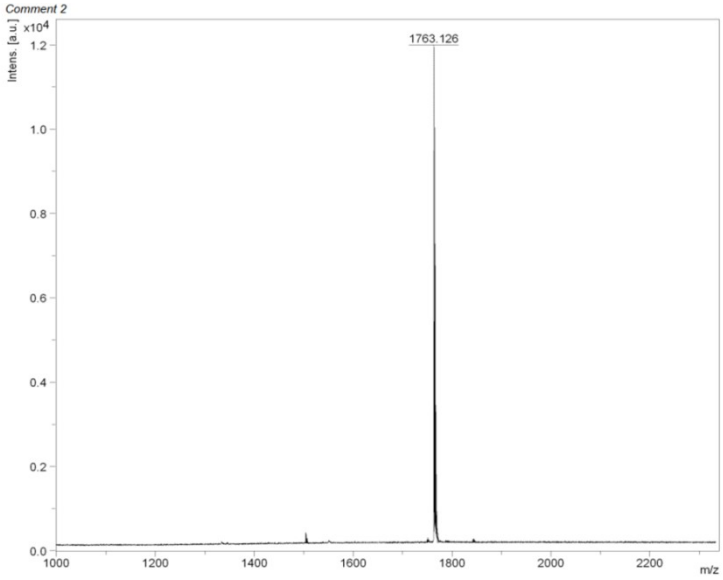

Fig. S4. MOLDI-TOF-MS spectrum of DPP-OPIC.

3. Characterizations of NPs

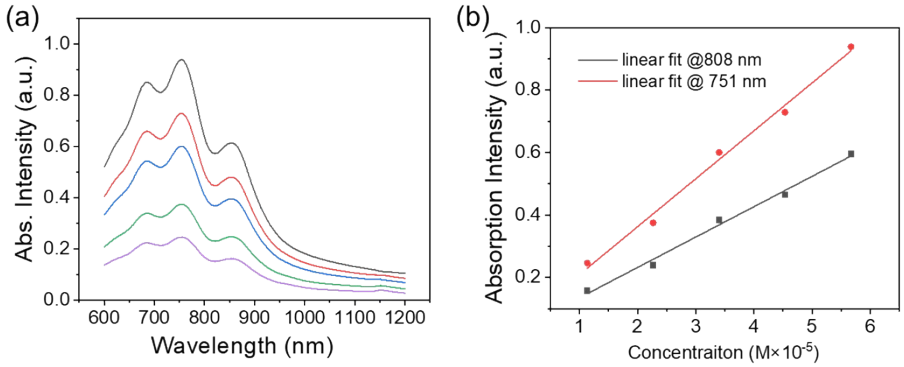

Fig. S5. (a) Absorption spectra of DPP-OPIC NPs with different concentrations. (b) The linear function of absorbance intensity versus concentration.

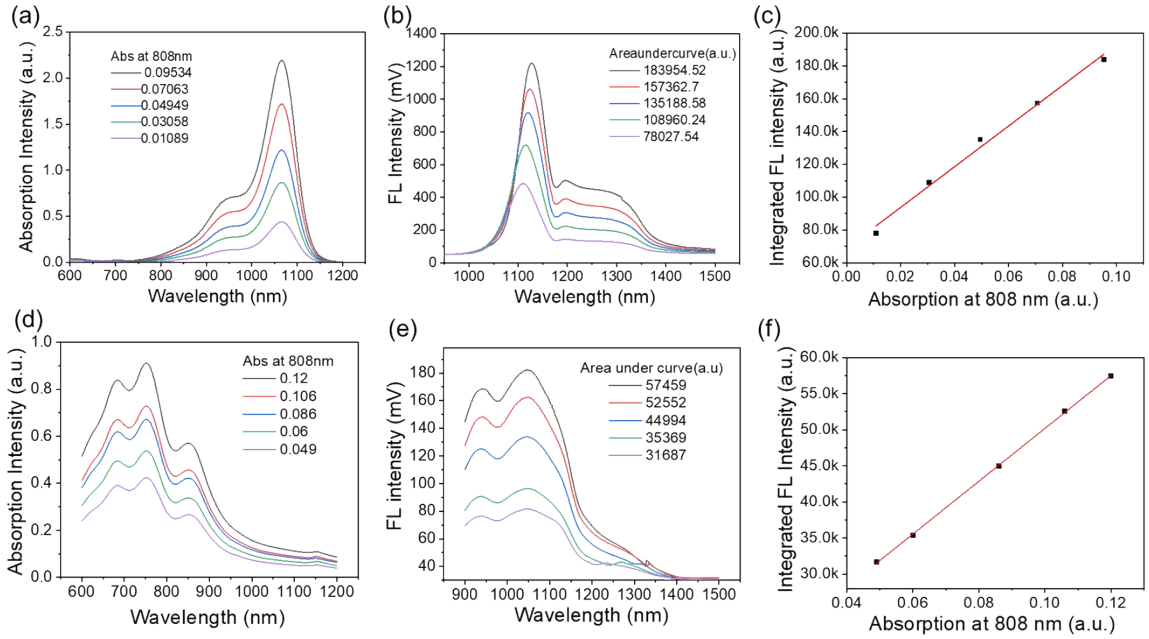

Fig. S6. (a) The absorption spectra of IR-1061 in DEM with different concentrations. (b) The emission spectra of IR-1061 in DEM with different concentrations. (c) The linear fitting function of absorbance values versus integrated area of fluorescence spectra. (d), (e) and (f) The data for DPP-OPIC NPs using the same measurement and calculation process.

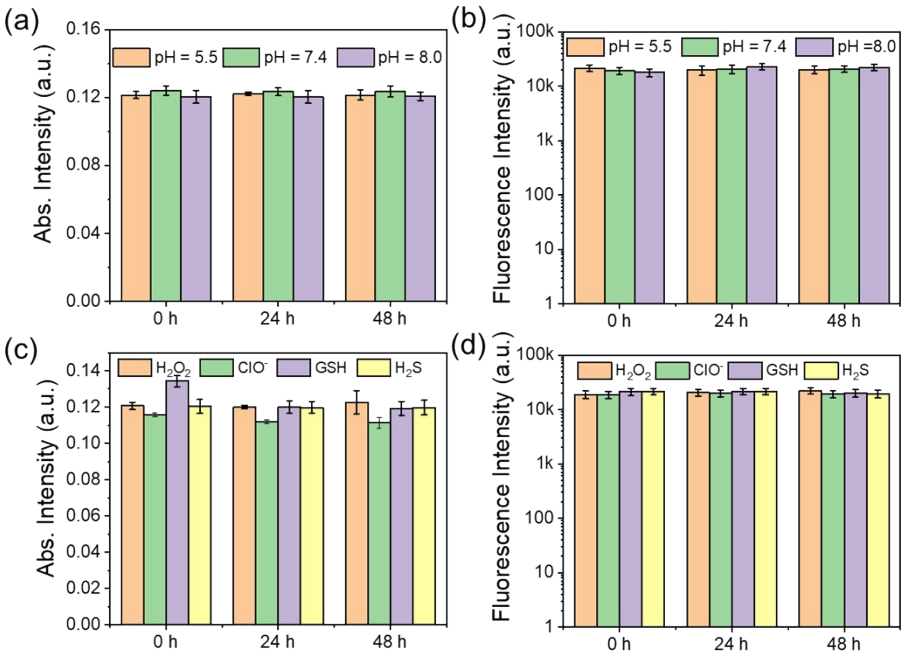

Fig. S7. Changes at absorbance (at 808 nm) (a) and fluorescence intensity (b) of DPP-OPIC NPs in various pH values; Changes at absorbance (at 808 nm) (c) and fluorescence intensity (d) of DPP-OPIC NPs added with H_2O_2, ClO^-, GSH and H_2S (10^{-4} M).

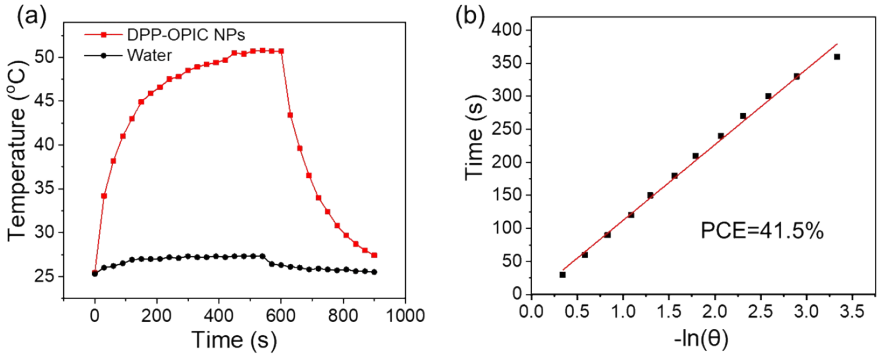

Fig. S8. Heating and cooling curves of DPP-OPIC NPs. (b) Linear fitting of cooling time versus -ln(θ) obtained from (a).

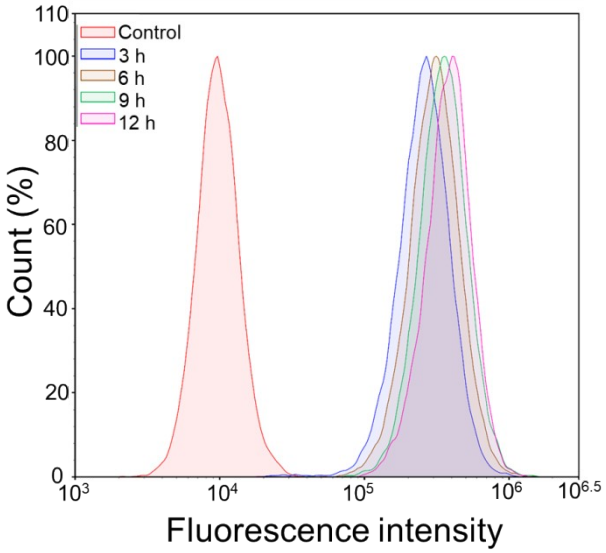

Fig. S9. Flow cytometry analysis for cellular uptake of DPP-OPIC NPs assays.

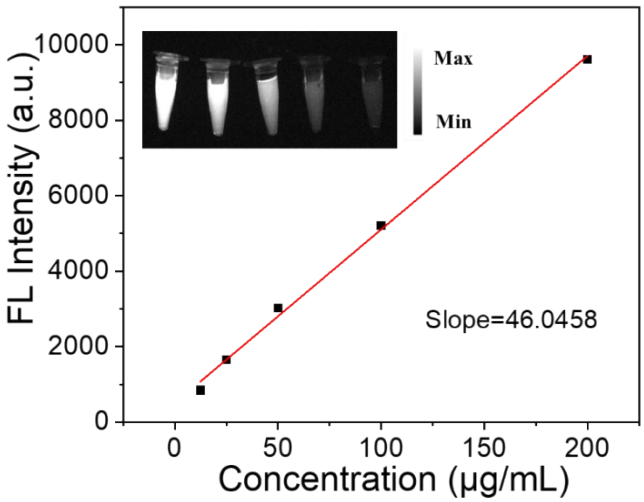

Fig. S10. Fluorescence intensity of DPP-OPIC NPs with various concentrations and related linear.

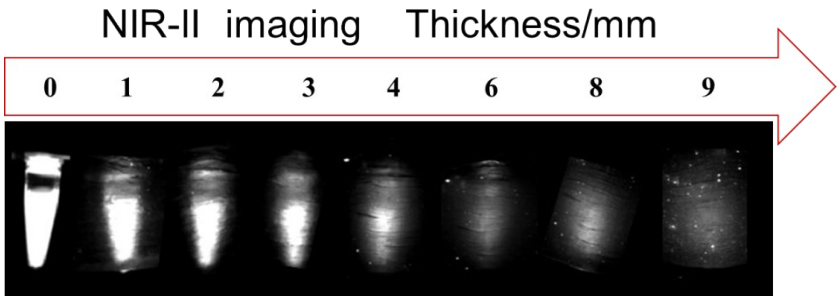

Fig. S11. The experiment of penetration depth of DPP-OPIC NPs under 808 nm laser irradiation.